Histol Histopathol (2004) 19: 1141-1151

http://www.hh.um.es

Histology and Histopathology

Cellular and Molecular Biology

Pathological changes in the liver of a senescence accelerated mouse strain (SAMP8): A mouse model for the study of liver diseases

X. Ye, H.C. Meeker, P.B. Kozlowski, J. Wegiel, K.C. Wang, H. Imaki and R.I. Carp

NYS/Institute for Basic Research in Developmental Disabilities, Staten Island, NY, USA

Summary. Liver disease is characterized by fatty liver, hepatitis, fibrosis and cirrhosis and is a major cause of illness and death worldwide. The prevalence of liver diseases highlights the need for animal models for research on the mechanism of disease pathogenesis and efficient and cost-effective treatments. Here we show that a senescence-accelerated mouse strain (SAMP8 mice), displays severe liver pathology, which is not seen in senescence-resistant mice (SAMR1). The livers of SAMP8 mice show fatty degeneration, hepatocyte death, fibrosis, cirrhotic changes, inflammatory mononuclear cell infiltration and sporadic neoplastic changes. SAMP8 mice also show abnormal liver function tests: significantly increased levels of alanine aminotransferase (ALT) and aspartate aminotransferase (AST). Furthermore, titers of murine leukemia virus are higher in livers of SAMP8 than in those of SAMR1 mice. Our observations suggest that SAMP8 mouse strain is a valuable animal model for the study of liver diseases. The possible mechanisms of liver damage in SAMP8 mice are also discussed.

Key words: SAMP8, Fatty liver, Fibrosis, ALT, AST

Introduction

The senescence accelerated mouse (SAM) strains were developed by Dr. Toshio Takeda and colleagues (Takeda et al., 1991; Takeda, 1999). These mice provide an excellent model system to study the processes of aging. A number of lines of senescence prone (P-series; SAMP) mice have been developed. Of the senescence prone strains, the SAMP8 strain has a life span of approximately 50% of the life span of another line developed by the Takeda group, termed senescence resistant (R-series; SAMR1). In addition to the shorter life span, mice of the SAMP8 strain have a reduced capacity to learn and poor memory retention (Miyamoto et al., 1986). At an early age these mice show many of the histopathological signs associated with mice affected with neurodegenerative diseases or with aged normal mice, e.g., 2-year-old SAMR1 mice; in comparison to normal aging, the changes seen in SAMP8 are more intense.

We found that SAMP8 mice displayed extensive liver degeneration. Our findings were reproducible in SAMP8 mice harvested in different years (1995, 2001 and 2002) and liver degeneration was found in different age groups (10 months and 16 months). This is the first description of liver degeneration in SAMP8 mice. These findings have been confirmed by Dr. Y.S. Kim's group in Korea (personal communication). The plasma levels of alanine aminotransferase (ALT) and aspartase aminotransferase (AST) were significantly increased in SAMP8 mice compared to the values in SAMR1 mice. Testing of SAMP8 and SAMR1 livers for ecotropic murine leukemia virus (MuLV) showed a striking difference in virus titers: SAMP8 mice exhibited very high virus levels in liver compared to the levels in SAMR1. At this time, we are not sure if MuLV viruses in the liver of SAMP8 mice cause liver degeneration. Our findings provide a valuable animal model to study the mechanisms of liver disease and to test the efficiency of various treatment modalities.

Materials and methods

Animals

SAMR1/Ta and SAMP8/Ta strains were originally obtained from Dr. T. Takeda (Takeda et al., 1991; Takeda, 1999) and have been maintained as inbred strains in the Institute for Basic Research (IBR) animal colony since 1992. Pathogen-free SAMR1 and SAMP8 animals were obtained subsequently from Drs. J.F. Flood and J.E. Morley (Flood and Morley, 1994) and have been housed in Thoren cages in a clean facility separate from the main animal colony. The pathogen-free mice have been bled and checked serologically for common

Offprint requests to: Dr. Xuemin Ye, New York State Institute for Basic Research in Developmental Disabilities, 1050 Forest Hill Road, Staten Island, NY, 10314, USA. Fax: 718 698 0896. e-mail: XYE@hotmail.com

murine pathogens by the serological testing service of Charles River Laboratories. These mice have remained pathogen free. All mice were on a 12-hr light, dark cycle and fed and watered *ad libitum*.

At the time of harvest, more than seven animals in each group were anesthetized with 5 mg Nembutal i.p. Blood was taken before perfusion (between 10:00 am and 1:00 pm) from the heart and collected in labeled polyethylene tubes. Plasma was stored at 4 °C for later plasma assays. Mice were perfused transcardially with cold phosphate-buffered saline (PBS) followed by cold 4% paraformaldehyde in PBS. The livers were immediately removed, cut into blocks, postfixed overnight in the same fixative at 4 °C, then processed as described for electron microscopy studies or rinsed with PBS, dehydrated with ethanol and embedded in polyester wax (Polyscience, USA) for light microscopy studies. Some mice were perfused with ice-cold physiological saline (PS); unfixed livers were immediately removed from these mice. Parts of each liver were cut into 20 µm-thick sections in a cryostat for frozen sections and the remaining portions were homogenized with 10 mM HEPES buffer (pH 7.4) for later use.

Histological staining

Tissue blocks were processed into paraffin blocks and sectioned into 7 µm-thick histological sections. The sections of liver and other organs were stained with haematoxylin and eosin (HE). Frozen liver sections, 20 µm thick, were stained with Sudan black or oil red for examination of fat distribution. Necrosis and other abnormalities detectable by light microscopy were assessed in histological preparations previously coded in order at avoid bias. Tissue necrosis was scored as follows: 0, no necrosis; 1+, focal necrosis of few cells per section; 2+, focal necrosis of many cells per section; 3+, areas of massive confluent necrosis; 4+, zonal massive necrosis.

Transmission electron microscope (TEM)

After immersion-fixation in 2% glutaraldehyde and 2% paraformaldehyde in cacodylate buffer overnight at 4 °C, the livers were rinsed four times 5 min each in 0.1 M cacodylate buffer. The livers were trimmed so that the size of the tissue was about $1mm^3$. The tissue was post-fixed in 1% osmic acid in cacodylate buffer for 30 minutes, and then it was rinsed twice in 0.1 M cacodylate buffer and once in 1% tannic acid for 1 hour. The specimens were rinsed twice in the buffers and were dehydrated in increasing concentrations of alcohol, from 30% up to 100%. The specimens were then infiltrated with Epon embedding medium and were polymerized in an oven at 60 °C for several days before sectioning. Ultra-thin sections were stained with uranyl acetate and lead citrate. The specimens were observed with a transmission electron microscope (Hitachi 7000).

Liver function tests

The levels of ALT (EC 2.6.1.2), AST (EC 2.6.1.1), and alkaline phosphatase (AP) (EC 3.1.3.1) in the plasma were measured by use of kits purchased from Sigma (USA); the manufacturer's instructions have been modified to use small volumes in a 96-well Corning plate (Fisher), and we have shown that this modified procedure is effective in obtaining the expected standard curves.

MuLV assay

Perfusion of mice and liver homogenates preparation

Four mice in each group were anesthetized with 5 mg sodium pentobarbital (Nembutal) i.p. and sprayed liberally with 70% ethanol. When mice were unconscious but had an active heartbeat, mice were perfused with sterile PBS through the left ventricle for 10 min. After perfusion, livers were removed aseptically and processed by homogenization in DMEM (10% w/v), using 20 strokes in a hand-operated, ground-glass tissue homogenizer. Serial dilutions of liver homogenates were prepared in DMEM + 10% FBS + 100u/ml penicillin-100mg/ml streptomycin + 25 µg/mL DEAE-dextran (DMEM10A-DEAE).

Culture of cell lines

SC-1 cells (ATCC CRL-1404) were grown in Dulbecco's modified eagle medium (DMEM) + 10% fetal bovine serum (FBS) + 100 µg/mL penicillin + 100 µg/mL streptomycin (DMEM10A). The XC cell line (ATCC CCL-165) was grown in DMEM + 10% FBS without antibiotics (DMEM10). SC-1 and XC cells were harvested for use in plaque assays by trypsin-EDTA (0.05% trypsin, 0.53 mM EDTA; 1 ml of this trypsin-EDTA solution/$25cm^2$ flask), washed once with DMEM, and resuspended in the appropriate medium for assay. All cell-growth and plaque assays were done at 37 °C in a humidified, 5% CO_2 incubator (Carp et al., 1999).

SC-1 UV plaque assay

Ecotropic MuLV was quantitated using the SC-1/UV plaque assay (Rowe et al., 1970; Meeker and Carp, 1997). SC-1 cells were plated onto 60 mm plastic Petri dishes at 10^5 cells per dish in 4 ml DMEM10A. The next day, approximately 1 h before addition of liver homogenates, medium in the dishes was discarded and replaced with 3 ml DMEM + 10% FBS + 100u/ml penicillin-100mg/ml streptomycin + 25 µg/mL DEAE-dextran (DMEM10A-DEAE). One ml volume of liver homogenate diluted in the same medium was then added to plates. One to two days after addition of liver homogenate, medium was removed and replaced with 4 ml per dish DMEM10A. Five days after addition of liver homogenate, medium was removed and cultures were

exposed to 30 s of UV irradiation. Immediately after UV irradiation, 4 ml of a suspension containing $2.5x10^5$ XC cells/ml in DMEM10A was pipetted into each dish. After 24 h incubation, medium was discarded. Cultures were washed once with PBS, fixed with 100% methanol for 5 min and stained with haematoxylin for 10 min. Haematoxylin was discarded, the cultures washed twice with tap water, and the plaques counted under a dissecting microscope. Concentrations of liver homogenates higher than 1 ml of 1% (w/v) in 4 ml culture medium were found to be toxic to SC-1 cells. Therefore, liver homogenates were diluted in serial tenfold dilutions with 1% the highest concentration used. MuLV titres were expressed as log10 PFU/mg liver.

Statistical analysis

All the data were processed and stored in computer (Dell, Dimension L866r). Statistical differences between groups were assessed by Student's t-test or analysis of variance using the Instat statistical program (GraphPAD Software, San Diego, CA). Acceptable statistical significance was set at $p<0.05$.

Results

SAMP8 and SAMR1 mice used in this study were shown in Figure 1A. The SAMP8 mouse exhibited generalized signs of aging, which included ruffled and dull coat, loss of hair, abnormal curvature of the spine and inflammation in the periorbital areas. Hematoxylin and eosin (HE)-stained sections of livers in SAMR1 mice were essentially normal (Fig. 1B). Only minor liver vacuolation was found in less than 10% of SAMR1 mice. These changes could be considered non-pathological. However, there was extensive fatty degeneration in the livers of SAMP8 mice (Fig. 1C). The characteristic feature of liver injury in SAMP8 mice was the predominance of steatosis and other lesions in the perivenular area (also called centrilobular zone or zone 3) of the hepatic acinus. Portal and periportal regions were normal (Fig. 1C). Steatosis was present predominantly as macrovesicular fat; some hepatocytes had an admixture of microvesicular steatosis (Fig. 1D). The nuclei were centrally located and of normal size. In HE stained slides and Sudan black stained slides, lipid droplets were found in the livers of SAMP8 mice (Figs. 1F and 1G), but not in the livers of SAMR1 mice (Fig. 1H).

Higher power magnification of the centrilobular region of SAMP8 livers showed hepatocellular degeneration, with enlarged or pyknotic liver cell nuclei, swelling cell bodies and necrosis with deposition of cell debris. Activation of cells of the reticular endoplasmic system plus infiltration of lymphocytes and leukocytes could also be seen. Under high power (magnification see Figure Captions), livers showed fatty change, hepatocyte ballooning characterized by swollen cells, focal necrosis, fibrosis and focal inflammatory infiltrates in midzonal and centrilobular regions. Necrosis was limited to the centrilobular zone, and was accompanied by centrilobular swelling of cells, polymorphonuclear leukocytic infiltration, fibrosis and cell degeneration (Figs. 2A-G). The possibility existed that (1) there was a gradient of decreasing oxygen tension from the portal to the central venous end of the sinusoid, and/or (2) there was a gradient of increased aging of hepatocytes from the portal areas to the central areas due to hepatocytic proliferation which starting in portal areas. Therefore, the cells around the centrilobular zone were more vulnerable to the damage. Sporadically, SAMP8 mice developed hepatic neoplasm-like proliferation with fibrosis and leukocytic infiltration (Fig. 2D,G).

In SAMP8 mice, the lipid droplets in the liver cells ranged in size up to 8 to 10 µm in diameter, but most of the droplets averaged 1.5 to 3.5 µm under electron microscopic examination. There was a general tendency for the droplets to be distributed near the sinusoidal borders of the liver cells (Fig. 3A), but they could be found in all portions of the cytoplasm (Fig. 3B). Smooth endoplasmic reticulum, the granular endoplasmic reticulum and mitochondria were normal in some areas, but showed changes such as degeneration in the areas of necrosis. The smooth endoplasmic reticulum was widely distributed in the centrilobular cells, scattered among the vesicles (Fig. 3A,B, see arrows). Groups of activated macrophages and lymphocytes were found between liver cells (Fig. 3C); sometimes they were found near the Kupffer cells (Fig. 3D). Connective tissue was found in Disse space near the stellate cells in the damaged areas. The connective tissue was found laid down in the perivascular space around the central vein and in the perisinusoidal region (Fig. 3E). The fatty degeneration was found in both young (10 months old) and old (16 months old) SAMP8 mice (Fig. 4). The vacuolation scores were significantly higher in SAMP8 mice than those in SAMR1 mice. In young SAMR1 mice, the vacuolation score was 0.83±0.54 (n=6) and in old SAMR1 mice it was 0.22±0.16 (n=27), while the vacuolation score in young SAMP8 mice was 3.00±0.33 (n=10) and in old SAMP8 mice it was 1.74±0.32 (n=23).

SAMP8 mice also showed abnormal liver function tests in two different age groups (10 months and 16 months). The plasma ALT levels (Sigma units/ml) in SAMP8 mice were significantly increased compared to those in SAMR1 mice. In young SAMR1 mice, the plasma ALT level was 33.3±3.6 (n=17) and in old SAMR1 mice it was 41.8±11.3 (n=18), while the plasma ALT level in young SAMP8 mice was 127.0±28.7 (n=27) and in old SAMP8 mice it was 129.7±29.1 (n=22).

The plasma AST levels (Sigma units/ml) in SAMP8 mice were also significantly increased more than those in SAMR1 mice. In young SAMR1 mice, the plasma AST level was 81.8±14.6 (n=15) and in old SAMR1 mice was 87.4±5.8 (n=18), while the plasma AST level in young SAMP8 mice was 128.1±14.4 (n=27) and in old SAMP8 mice it was 148.7±26.8 (n=22).

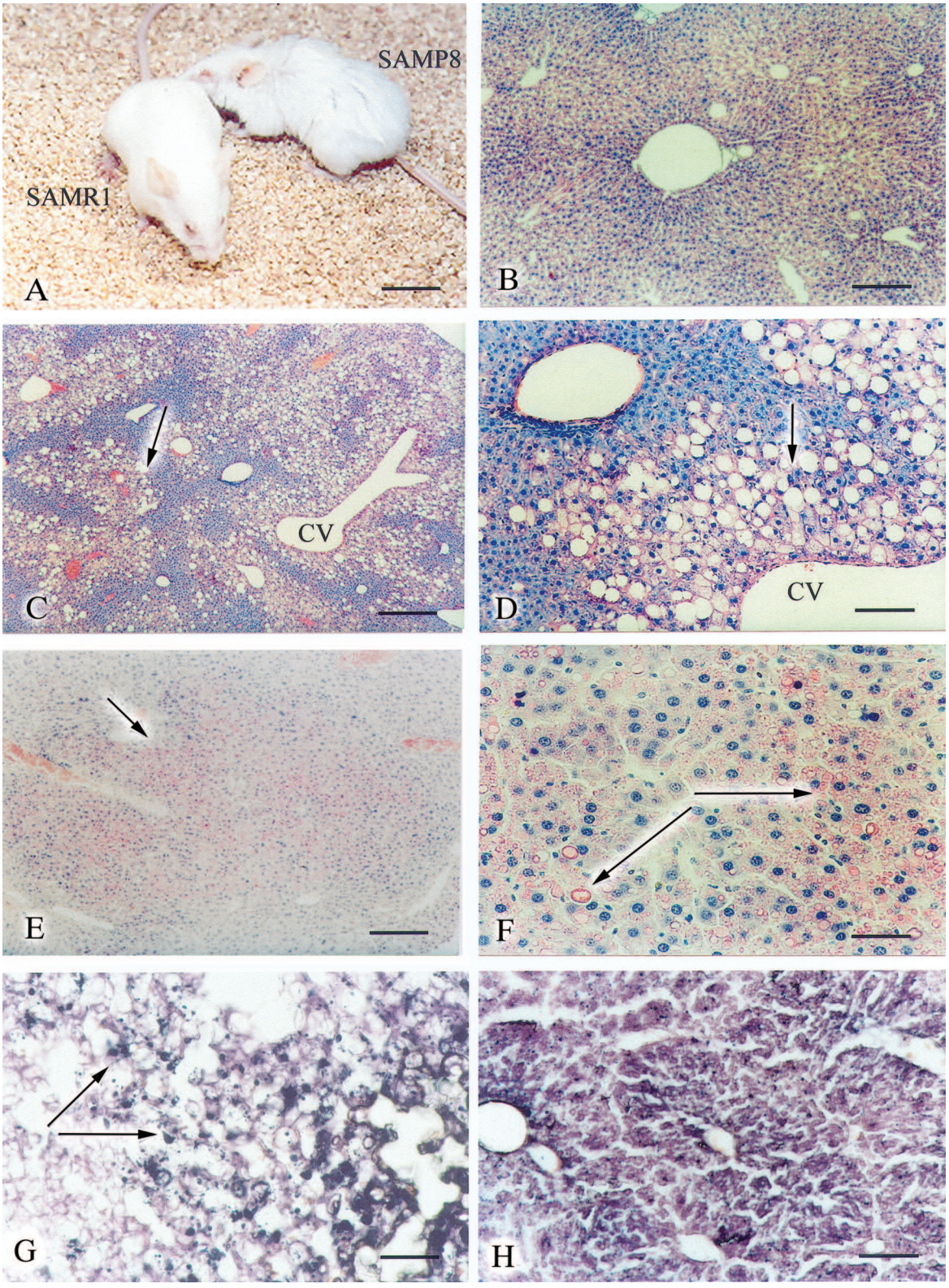

Fig. 1. A. Photo of SAMP8 and SAMR1 mice, both are 12 months old. **B.** Liver of SAMR1 mouse, HE stain. **C-F**. Fatty degeneration changes in the livers of SAMP8 mice, HE stain, arrows show fatty degeneration. **G.** Fatty droplets (arrows) in the liver of SAMP8 mouse, Sudan black stain. **H.** The liver of SAMR1 mouse, Sudan black stain. CV: central vein. Scale Bars: A, 2 cm; B, C, E, G, H, 220 μm; D, F, 110 μm.

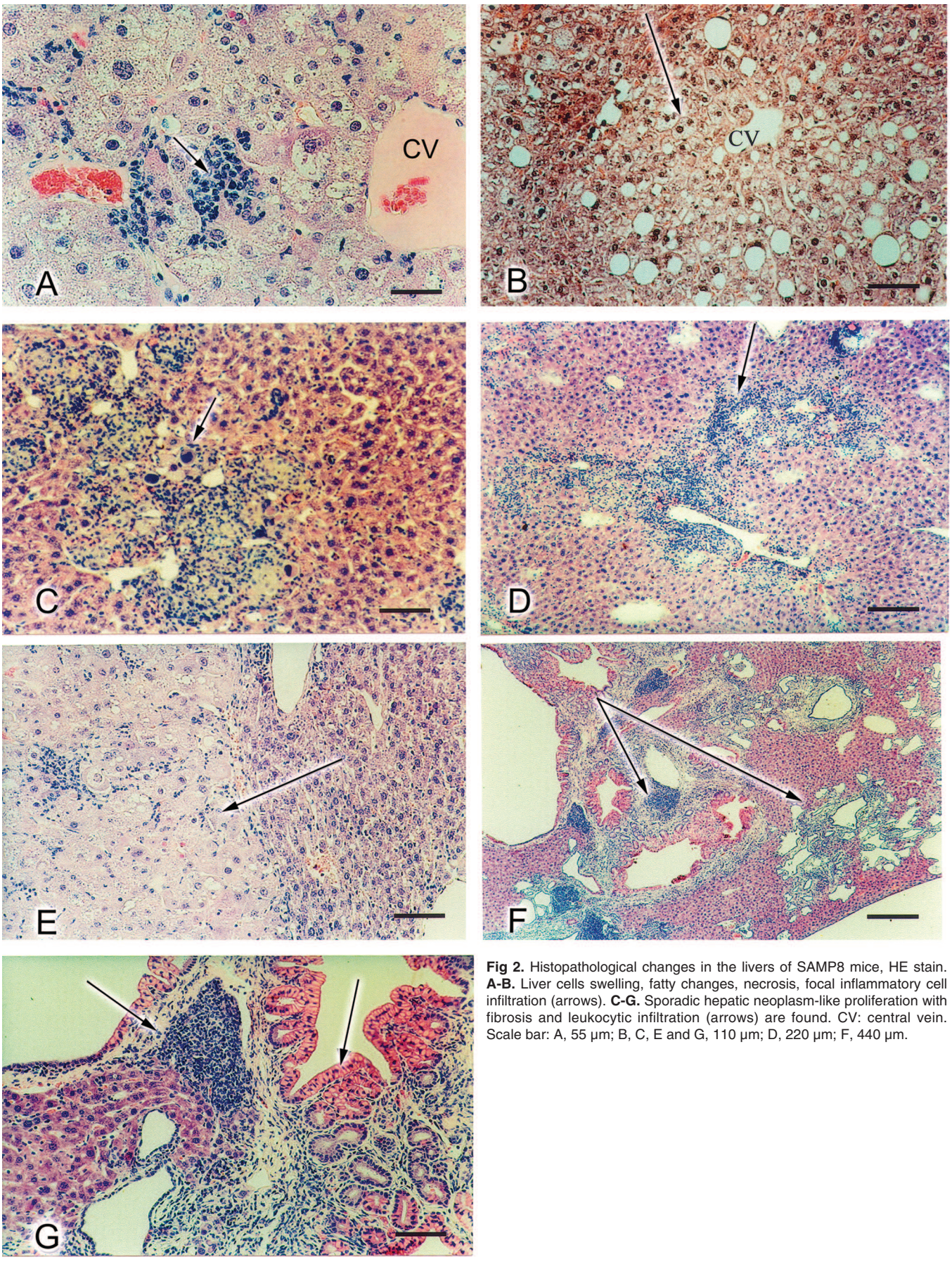

Fig 2. Histopathological changes in the livers of SAMP8 mice, HE stain. **A-B.** Liver cells swelling, fatty changes, necrosis, focal inflammatory cell infiltration (arrows). **C-G.** Sporadic hepatic neoplasm-like proliferation with fibrosis and leukocytic infiltration (arrows) are found. CV: central vein. Scale bar: A, 55 μm; B, C, E and G, 110 μm; D, 220 μm; F, 440 μm.

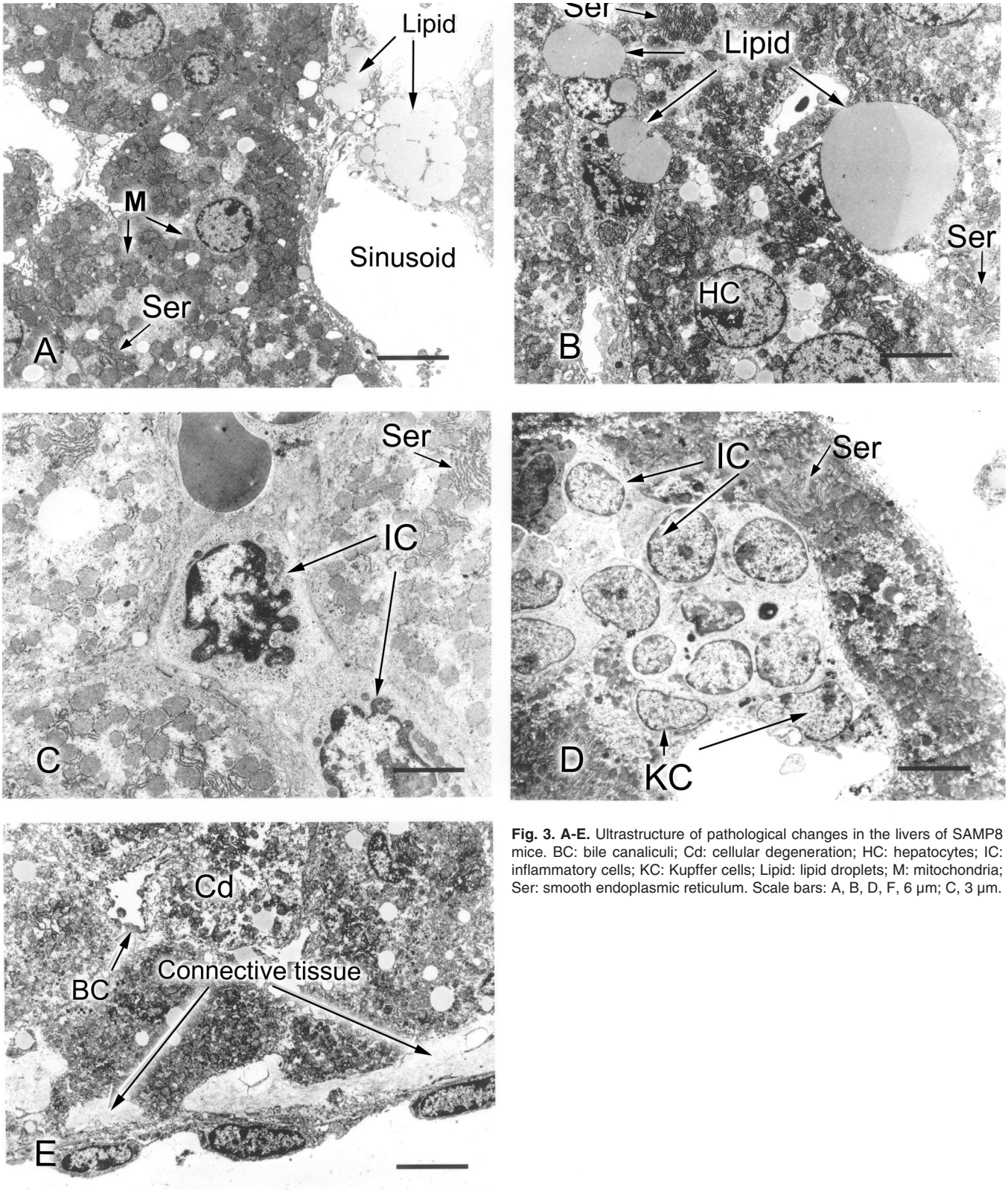

Fig. 3. A-E. Ultrastructure of pathological changes in the livers of SAMP8 mice. BC: bile canaliculi; Cd: cellular degeneration; HC: hepatocytes; IC: inflammatory cells; KC: Kupffer cells; Lipid: lipid droplets; M: mitochondria; Ser: smooth endoplasmic reticulum. Scale bars: A, B, D, F, 6 µm; C, 3 µm.

The plasma AP levels (Sigma units/ml) in SAMP8 mice were slightly increased compared to those in SAMR1 mice. In young SAMR1 mice, the plasma AP level was 2.9±0.2 (n=17) and in old SAMR1 mice it was 2.9±0.1 (n=17), while the plasma AP level in young SAMP8 mice was 3.1±0.2 (n=26) and in old SAMP8 mice was 3.3±0.2 (n=22).

Figures 5, 6 showed that ALT and AST were increased significantly, while alkaline phosphatase (AP) (Fig. 7) was slightly increased in SAMP8 mice compared to the values in SAMR1 mice.

There were higher MuLV titers in the livers of SAMP8 mice. SAMR1 exhibited very low virus levels in livers (0.9±0.1 $\log_{10}$ PFU/1 mg liver tissue) as compared to much higher levels in SAMP8 (2.7±0.2, $\log_{10}$ PFU/1 mg liver tissue) ($p<0.0001$) (Fig. 8).

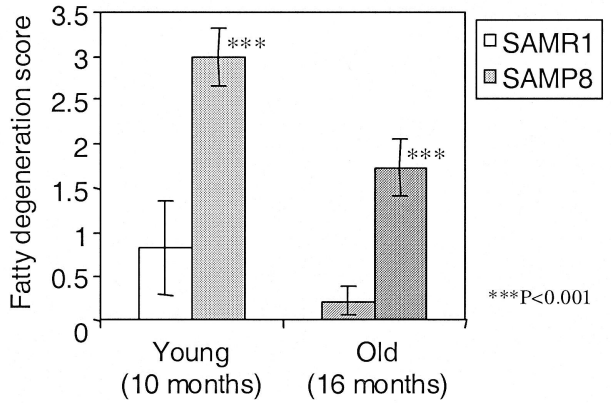

Fig. 4. Comparison of vacuolation (Fatty Liver) scores in SAMR1 and SAMP8 mice.

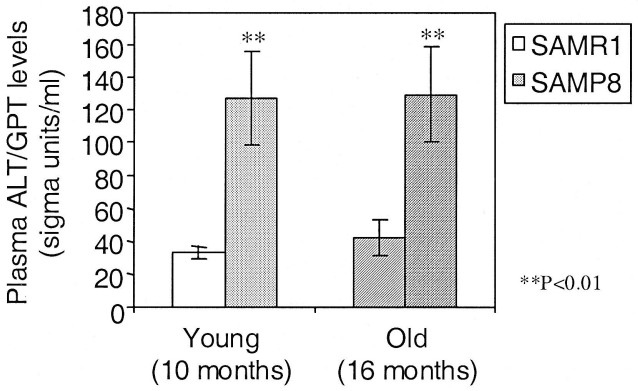

Fig. 5. Comparison of Plasma ALT Levels (Sigma units/ml) in SAMR1 and SAMP8.

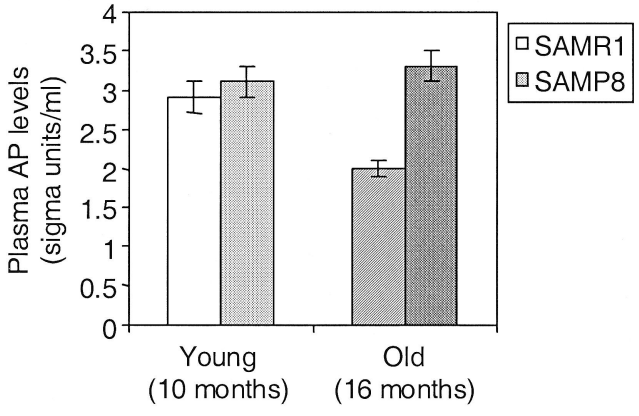

Fig. 7. Comparison of Plasma AP Levels (Sigma units/ml) in SAMR1 and SAMP8.

Discussion

This is the first report that demonstrates that a short-lived inbred mouse strain termed senescence-accelerated

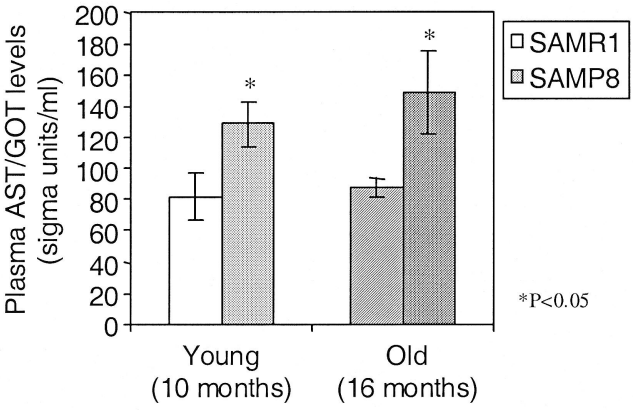

Fig. 6. Comparison of Plasma AST Levels (Sigma units/ml) in SAMR1 and SAMP8.

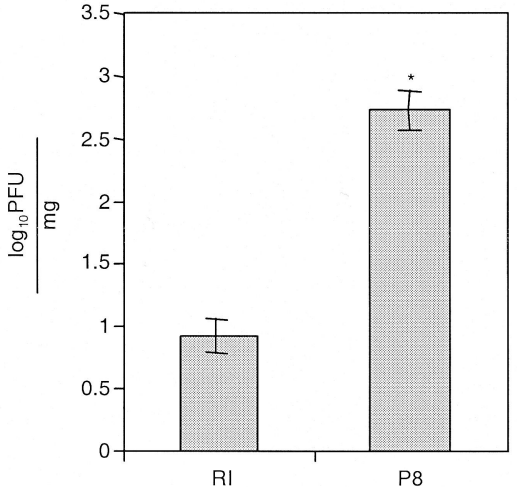

Fig. 8. Comparison of MuLV levels in the livers of SAMP8 and SAMR1 mice. *: $p<0.0001$.

mice (SAMP8) displays liver disease. In contrast, another strain with a normal aging process, referred to as senescence-resistant strain (SAMR1), did not display liver damage. The characteristic features of liver damage in SAMP8 mice are found predominantly in the perivenular area (also called centrilobular zone or zone 3) of the hepatic acinus. In this area, the livers show vacuolation, cell swelling and in some cases, lymphocytic infiltration. Higher power magnification of the centrilobular regions shows hepatocellular necrosis, and pyknotic liver cell nuclei. The pathological changes in the liver of SAMP8 mice are very similar to the ethanol-induced pathological changes seen in rat liver. Viral infection, alcoholic or drug toxicity, and many other factors that cause damage to hepatocytes elicit an inflammatory reaction in the liver (Wu and Zern, 2000).

Furthermore, SAMP8 mice also show abnormal liver function tests: the activity of ALT, AST and AP are increased in SAMP8 mice compared to the values in SAMR1 mice. The levels of AST and ALT are increased in conditions where the liver has been inflamed or liver cells are dying. As the cells are damaged, the AST and ALT leak into the bloodstream leading to a rise in serum levels. Plasma levels of ALT and AST rise rapidly during the early stages of liver disease. Our study shows significant increases in AST and ALT levels in SAMP8 mice compared to SAMR1 mice. These results suggest that the liver cells of SAMP8 mice have undergone cell damage and cell necrosis.

AP is actually a group of enzymes that hydrolyze monophosphate esters at an alkaline pH. AP is associated with the biliary tract. Liver disease resulting in parenchymal cell necrosis does not elevate plasma alkaline phosphatase unless the liver disease is associated with damage to the canaliculi or with biliary stasis.

The mechanism of liver degeneration in SAMP8 mice is still not known. One possibility is the higher MuLV titers in the livers of SAMP8 mice. SAMP8 mice had approximately 50 times as much MuLV in livers compared to SAMR1 mice (Fig. 8). It has been reported that the titers of MuLV are higher in brains of SAMP8 than SAMR strains (Meeker and Carp, 1997; Carp et al., 2002). MuLVs are retroviruses, RNA tumor viruses that use reverse transcriptase to produce a DNA copy of the viral genome. This DNA can become integrated into the host genome as a provirus (Rowe et al., 1970; Rowe, 1972) and can replicate with the host chromosomal DNA. This provirus, referred to as endogenous, can be either replication-competent or replication-defective (Temin, 1992). A number of MuLVs are known to replicate and cause disease in the central nervous system (Sharpe et al., 1990; Wong, 1990; Kay et al., 1991; Czub et al., 1992; Hoffman et al., 1992). Although there is no evidence that MuLV causes liver degeneration in SAMP8 mice, viruses such as hepatitis A, B, and C do cause liver degeneration in humans (Beard and Lemon, 1999; Robinson, 1999; Purcell, 1999).

It has been found that there are age-related changes in liver function, including adverse drug reactions (Le Couteur and McLean, 1998), increased susceptibility to neurotoxins (Le Couteur et al., 2002a,b, Yang et al., 2002), and the appearance of atherosclerosis (Le Couteur et al., 2002a). Furthermore, it has been found that ageing in the liver is associated with reductions in mass and blood flow in the order of 30-50% (Le Couteur and McLean, 1998; Schmucker, 1998). In old rats, non-human primates and humans, marked changes were found in the hepatic sinusoidal endothelium and extracellular space of Disse, a condition that is termed pseudocapillarization (Le Couteur et al., 2001; Cogger et al., 2003; McLean et al., 2003).

It has been suggested that microvascular abnormalities are found in ageing liver (McLean et al., 2003). By electron microscopic analysis, ageing was shown to be associated with a 50% increase in thickness of the endothelium and a 50% reduction in the number of fenestrations in the sinusoidal endothelium (Le Couteur et al., 2002a). Immunocytochemistry studies showed strong expression of collagen IV, moderate expression of factor VIII-related antigen, and weak expression of collagen I along the sinusoids of livers from old rats (Le Couteur et al., 2001). Thickening of the endothelium and deposition of extravascular collagen might impair the transfer by diffusion of substrates such as oxygen (Le Couteur et al., 2001) and drugs (Fenvyes et al., 1993). In the current study, the sinusoidal ageing phenomenon might be linked to the centri-lobular pattern of the lesions via the mechanism of hypoxia. It would be interesting to determine if there were similar sinusoidal ageing changes in the livers of SAMP8 mice.

Another possible cause of liver degeneration in SAMP8 mice is oxidative stress, which has been reported to play a key role in pathogenesis of liver disease. There is evidence for intrahepatocytic hypoxia in aged rats (Le Couteur et al., 2001). In the study of oxidative stress in the brain and peripheral organs in both SAMP8 and SAMR1 mice, it has been found that the level of lipid peroxides in the brain did not show an age-dependent change, but at each age the brain level of lipid peroxides was significantly higher in SAMP8 than in SAMR1. In contrast, the lipid peroxide levels in heart; liver, lung and kidney showed increases with aging in both SAMP8 and SAMR1 mice (Matsugo et al., 2000). Furthermore, this study showed lipid peroxide levels significantly higher in SAMP8 than in SAMR1. These results suggest that increased oxidative stress in the brain and peripheral organs may be a cause of the senescence-related degeneration and impairment seen in the brain and liver of SAMP8.

Free radicals produced by metabolic pathways promote progression from steatosis to steatohepatitis and fibrosis by three main mechanisms: lipid peroxidation, cytokine induction, and Fas ligand induction (Angulo, 2002). It has been reported that aldehydes generated endogenously during the process of lipid peroxidation are causally involved in most of the pathophysiological effects associated with oxidative stress in cells and

tissues (Esterbauer et al., 1991). Among the lipid peroxidation-derived aldehydes, 4-hydroxy-2-nonenal (HNE) is believed to be largely responsible for the cytopathological effects observed during oxidative stress in vivo (Esterbauer et al., 1991; Fazio et al., 1992; Parola et al., 1993; Barrera et al., 1996; Rao et al., 1996; Spycher et al., 1996; Fukuda et al., 1997; Leonarduzzi et al., 1997; Uchida et al., 1999). HNE plays a role in inhibition of protein and DNA synthesis, inactivation of enzymes, stimulation of phospholipase C and reduction of gap-junction communication. Preliminary results suggest that HNE is increased in the livers of SAMP8 mice compared to SAMR1 mice and might play an important role in liver oxidative stress and liver pathology seen in this strain (unpublished).

The numbers 1-15 in the next 3 paragraphs list the possible mechanisms involved in liver degeneration induced by oxidative stress in SAMP8 mice. (1) It is possible that the genetic deficits and/or mutations in SAMP8 mice causes imbalance of oxidation-reduction reactions in the body; some nonalcoholic fatty livers might be caused by genetic deficits. (2) Reactive oxygen species (ROS) accumulate and trigger lipid peroxidation, which causes cell death and releases malondialdehyde (MDA) and HNE (Curzio et al., 1985; Esterbauer et al., 1991). (3) MDA and HNE might activate p38 and c-Jun N-terminal kinase (JNK) pathways. Therefore, (4) MDA and HNE stimulate stellate cells, promoting collagen synthesis (Leonarduzzi et al., 1997). (5) HNE has chemotactic activity for neutrophils, promoting tissue inflammation (Curzio et al., 1985). (6) ROS derived from parenchymal cells may signal nonparenchymal cell activation, including Kupffer and stellate cells, which can release inflammatory cytokines such as TNFα, transforming growth factor ß (TGFß), interleukin-8 (IL-8) and free radicals. TNFα inhibits mitochondrial electron transfer in target cells and induces oxidative stress in isolated mouse hepatocytes (Lancaster et al., 1989; Adamson and Billings, 1992). (7) It has been suggested that TNFα can increase circulating fatty acids and cause hyperinsulinemia (Angulo, 2002). (8) TNFα stimulates uptake of fatty acids by hepatocytes and leads to mitochondrial ß-oxidation overload. Lipid peroxidation also causes oxidation of low-density lipoprotein (LDL) and subsequent formation of lipid droplets, and fatty acid accumulation that cause fatty liver (Angulo, 2002). (9) ROS produced from mitochondria and cytosol can stimulate NFκB and increase TNFα formation, which causes a ˝snow-ball effect˝. (10) All of the above may cause cell degeneration and impair liver function (including abnormal changes of ALT and AST). (11) ROS can influence the flow of electrons along the respiratory chain in mitochondria (Lancaster et al., 1989); this inhibits ATP synthesis, causing necrosis. (12) TNFα and TGFß have been reported to cause activation of caspases and liver cell death (apoptosis or necrosis) (Inayat-Husain et al., 1997). (13) MDA and HNE in liver cells can cause depletion of GSH, increase peroxynitrite and lead to more ROS formation. Peroxynitrite is a strong oxidant and nitrating agent, which can promote lipid peroxidation and nitration of tyrosine residues on proteins (Beckman et al., 1990). (14) ROS in mitochondria can cause expression of the Fas ligand (Fas-L) in hepatocytes (Hug et al., 1997), which can then interact with Fas receptors on the membranes either by autocrine effect, which damages the cell itself or by paracrine processes, causing another cell's death. On the other hand, TGFß activates type II receptor on stellate cells and stimulates the synthesis of collagen type I, leading to fibrosis (Leonarduzzi et al., 1997; Wu and Zern, 2000). (15) ROS can also cause damage to DNA (Ames et al., 1993). Oxidative damage to DNA is postulated to be an important contributor to aging and cancer. It is estimated that the number of oxidative hits to DNA per cell per day is about 100,000 in the rat and about 10,000 in the human. DNA-repair enzymes such as glycosylase, cannot efficiently remove all of the lesions formed (Guyton and Kensler, 1993). The form of DNA damage produced by ROS includes modification of all bases as well as the production of base-free sites, deletions, frame shifts, strand breaks, DNA-protein cross links and chromosomal rearrangements. A common site for point mutation is G-C base pairs. 8-Oxo-2'-deoxyguanosine and its corresponding base, 8-hydroxy-2'-deoxyguanosine (8-OHdG) are particularly useful markers of oxidative DNA damage because they represent approximately 5% of the total oxidized bases that are known to occur in DNA. Oxidation at C8 position of G changes the electronic properties of this DNA base, which results in structural and conformational alterations in G and mispairing of G with A (Guyton and Kensler, 1993). The sporadic hepatic cancer found in SAMP8 mice might be the result of increased oxidative stress on DNA.

At present, we do not know what kind of genetic deficits and/or mutations exist in SAMP8 mice. In future experiments, we will measure the enzyme activities related to oxidative stress. We will also test the relationship of MuLV viruses, TNFα, lipid peroxidation, cytokine induction and Fas ligand induction to the liver degeneration process in SAMP8 mice.

Acknowledgements. This work was supported by New York State Institute for Basic Research in Developmental Disabilities. The authors thank Joanne Stocker for her excellent work in preparing this manuscript, Maureen Marlow for editing of this manuscript and Sharon Mathier for her help in the preparation of the figures and images.

References

Adamson G.H. and Billings R.E. (1992). Tumor necrosis factor induced oxidative stress in isolated mouse hepatocytes. Arch. Biochem. Biophys. 294, 223-229.

Ames B.N., Shigenaga M.K. and Hagen T.M. (1993). Oxidants, antioxidants, and the degenerative diseases of aging. Proc. Natl. Acad. Sci. USA 90, 7915-7922.

Angulo P. (2002). Nonalcoholic fatty liver disease. N. Engl. J. Med. 346, 1221-1231.

Barrera G., Pizzimenti S., Serra A., Ferretti C., Fazio V.M., Saglio G., and Dianzani M.U. (1996). 4-hydroxynonenal specifically inhibits c-myb but does not affect c-fos expressions in HL-60 cells. Biochem. Biophys. Res. Commun. 227, 589-593.

Beard M.R. and Lemon S.M. (1999). Hepatitis A virus (Picornaviridae). In: Encyclopedia of virology. Second edition. Granoff A. and Webster R.G. (eds). Academic Press. London. pp 631-639.

Beckman J.S., Beckman T.W., Chen J., Marshall P.A. and Freeman B.A. (1990). Apparent hydroxyl radical production by peroxynitrite: implications for endothelial injury from nitric oxide and superoxide. Proc. Natl. Acad. Sci. USA 87, 1620-1624.

Carp R.I., Meeker H.C., Caruso V. and Seren E. (1999). Scrapie strain-specific interaction with endogenous murine leukemia virus. J. Gen. Virol. 80, 5-10.

Carp R.I., Meeker H.C., Chung R., Kozak C.A., Hosokawa M. and Fujisawa H. (2002). Murine leukemia virus in organs of senescence-prone and -resistant mouse strains. Mech. Ageing Devel. 123, 575–584.

Cogger V.C., Warren A., Fraser R., Ngu M., McLean A.J. and Le Couteur D.G. (2003). Hepatic sinusoidal pseudocapillarization with aging in the non-human primate. Exp. Gerontol. 38, 1101-1107.

Curzio M., Esterbauer H. and Dianzani M.U. (1985). Chemotactic activity of hydroxyalkenals on rat neurotrophils. Int. J. Tissue React. 7, 137-142.

Czub M., McAtee F.J. and Portis J.L. (1992). Murine retrovirus-induced spongiform encephalomyelopathy: Host and viral factors which determine the length of the incubation period. J. Virol. 66, 3298-3305.

Esterbauer H., Schauer R.J. and Zollner H. (1991). Chemistry and biochemistry of 4-hydroxynonenal, maloaldehyde and related aldehydes. Free Radicals Biol. Med. 11, 81-128.

Fazio V.M., Barrera G., Martinotti S., Farace M.G., Giglioni B., Frati L., Manzari V. and Dianzani M.U. (1992). 4-Hydroxynonenal, a product of cellular lipid peroxidation, which modulates c-myc and globin gene expression in K562 erythroleukemic cells. Cancer Res. 52, 4866-4871.

Fenvyes D., Gariepy L. and Villeneuve J.P. (1993). Clearance by the liver in cirrhosis: I. Relationship between propranolol metabolism in vitro and its extraction by the perfused liver in the rat. Hepatology 17, 301-306.

Flood J.F. and Morley J.E. (1994). Studies on genetic aspects of impaired learning, memory in SAMP8 mice. In: The SAM model of senescence. Takeda T. (ed). Elsevier. Amsterdam. pp 405-408.

Fukuda A., Nakamura Y., Ohigashi H., Osawa T. and Uchida K. (1997). Cellular response to the redox active lipid peroxidation products: induction of glutathione S-transferase P by 4-hydroxy-2-nonenal. Biochem. Biophy. Res. Commun. 236, 505-509.

Guyton K.Z. and Kensler T.W. (1993). Oxidative mechanisms in carcinogenesis. Br. Med. Bull. 49, 523-544.

Hoffman P.M., Cimino E. F., Robbins D.S., Broadwell R.D., Powers J.M. and Ruscetti S.K. (1992). Cellular tropism and localization in the rodent nervous system of a neuropathogenic variant of Friend murine leukemia virus. Lab. Invest. 67, 314-321.

Hug H., Srand S., Grambihler A. Galle J., Hack V., Stremmel W., Krammer P.H. and Galb P.R. (1997). Reactive oxygen intermediates are involved in the induction of CD95 ligand mRNA expression by cytodstatic drugs in hepatoma cells. J. Biol. Chem. 272, 28191-28193.

Inayat-Hussain S.H., Couet C., Cohen G.M. and Cain K. (1997). Processing/activation of CPP32-like proteases is involved in transforming growth factor b1-induced apoptosis in rat hepatocytes. Hepatology 25, 1516-1526.

Kay D.G., Gravel C., Robitaille Y., and Jolicoeur P. (1991). Retrovirus-induced spongiform myeloencephalopathy in mice: Regional distribution of infected target cells and neuronal loss occurring in the absence of viral expression in neurons. Proc. Natl. Acad. Sci. USA 88, 1281-1285.

Lancaster J.R. Jr., Laster S.M. and Gooding L.R. (1989). Inhibition of target cell mitochondrial electron transfer by tumor necrosis factor. FEBS Lett. 248, 169-174.

Le Couteur D.G. and McLean A.J. (1998). The aging liver: drug clearance and an oxygen diffusion barrier hypothesis. Clin Pharmacokinet. 34, 359-373.

Le Couteur D.G., Cogger V.C., Markus A.M., Harvey P.J., Yin Z.L., Ansselin A.D. and McLean A.J. (2001). Pseudocapillarization and associated energy limitation in the aged rat liver. Hepatology 33, 537-543.

Le Couteur D.G., Fraser R., Cogger V.C. and McLean A.J. (2002a). Hepatic pseudocapillarisation and atherosclerosis in ageing. Lancet 359, 1612-1615.

Le Couteur D.G., Muller M., Yang M.C., Mellick G.D. and McLean A.J. (2002b). Age-environment and gene-environment interactions in the pathogenesis of Parkinson's disease. Rev. Environ. Health 17, 51-65.

Leonarduzzi G., Scavazza A., Biasi F., Chiarpotto E., Camandola S., Vogl S., Dargel R. and Poli G. (1997). The lipid peroxidation end product 4-hydroxy-2,3-nonenal up-regulates transforming growth factor beta1 expression in the macrophage lineage: a link between oxidative injury and fibrosclerosis. FASEB J. 11, 851-857.

Matsugo S., Kitagawa T., Minami S., Esashi Y., Oomura Y., Tokumaru S., Kojo S., Matsushima K. and Sasaki K. (2000). Age-dependent changes in lipid peroxide levels in peripheral organs, but not in brain, in senescence-accelerated mice. Neurosci. Lett. 278, 105-108.

McLean A.J., Cogger V.C., Chong G.C., Warren A., Markus A.M.A., Dahlstrom J.E. and Le Couteur D.G. (2003). Age-related pseudocapillarization of the human liver. J. Pathol. 200, 112-117.

Meeker H.C. and Carp R.I. (1997). Titers of murine leukemia virus are higher in brains of SAMP8 than SAMR1 mice. Neurobiol. Aging 18, 543-547.

Miyamoto M., Kiyoto Y., Yamazaki N., Nagaoka A., Matsuo T., Nagawa Y. and Takeda T. (1986). Age-related changes in learning and memory in the senescence-accelerated mouse (SAM). Physiol. Behav. 38, 399-406.

Parola M., Pinzani M., Casini A., Albano E., Poli G., Gentilini A., Gentilini P. and Dianzani M.U. (1993). Stimulation of lipid peroxidation or 4-hydroxynonenal treatment increases procollagen alpha 1 (I) gene expression in human liver fat-storing cells. Biochem. Biophys. Res. Commun. 194, 1044-1050.

Purcell R.H. (1999). Hepatitis C virus (Flaviviridae). In: Encyclopedia of virology. Second edition. Granoff A. and Webster R.G. (eds). Academic Press. London. pp 657-663.

Rao G., Glasgow W.C., Eling T.E. and Runge M.S. (1996). Role of hydroperoxyeicosatetraenoic acids in oxidative stress-induced activating protein 1 (AP-1) activity. J. Biol. Chem. 271, 27760-

27764.
Robinson W.S. (1999). Hepadnaviruses (Hepadnaviridae): Hepatitis B viruses. In: Encyclopedia of virology. Second edition, Granoff A. and Webster R.G. (ed). Academic Press. London. pp 640-650.
Rowe W.P. (1972). Studies of genetic transmission of murine leukemia virus by AKR mice. J. Exp. Med. 136, 1272-1286.
Rowe W.P., Pugh W.E. and Hartley J.W. (1970). Plaque assay techniques for murine leukemia virues. Virology 42, 1136-1139.
Schmucker D.L. (1998). Aging and the liver: an update. J. Gerontol. 53A, B315-B320.
Sharpe A.H., Hunter J.J., Chassler P. and Jaenisch R. (1990). Role of abortive retroviral infection in spongiform CNS degeneration. Nature 346, 181-183.
Spycher S., Tabataba-Vakili S., O'Donnell V.B., Palomba L. and Azzi A. (1996). 4-hydroxy-2,3-trans-nonenal induces transcription and expression of aldose reductase. Biochem. Biophys. Res. Commun. 226, 512-516.
Takeda T. (1999). Senescence-accelerated mouse (SAM): a biogerontological resource in aging research. Neurobiol. Aging 20, 105-110.
Takeda T., Hosokawa M. and Higuchi K. (1991). Senescence-accelerated mouse (SAM): a novel murine model of accelerated senescence. J. Am. Geriatric Soc. 59, 911-919.
Temin H.M. (1992). Origin and general nature of retroviruses. In: The retroviridae. Vol. 1. Levy J.A. (ed). Plenum Press. New York. pp 15–22.
Uchida K., Shiraishi M., Naito Y., Torii Y., Nakamura Y. and Osawa T. (1999). Activation of stress signaling pathways by the end product of lipid peroxidation. J. Biol. Chem. 274, 2234-2242.
Wong P.K.Y. (1990). Moloney murine leukemia virus temperature sensitive mutants: A model for retrovirus-induced neurological disorders. Curr. Top. Microbiol. Immunol. 160, 29-60.
Wu J. and Zern M.A. (2000). Hepatic stellate cells: a target for the treatment of liver fibrosis. J. Gastroenterol. 35, 665-672.
Yang M.C., McLean A.J. and Le Couteur D.G. (2002). Age-related alteration in hepatic disposition of the neurotoxin 1-methyl-4-phenyl-1,2,3,6-tetrahydropyridine and pesticides. Pharmacol. Toxicol. 90, 203-207.

Accepted May 14, 2004